Measuring myocardial motion changes in tagged MR to establish inverse electro-mechanical coupling for XMR-guided RF ablation

Gerardo I. Sanchez-Ortiz[1], Maxime Sermesant[2],
Raghavendra Chandrashekara[1], Kawal S. Rhode[2],
Reza Razavi[2], Derek L.G. Hill[2], and Daniel Rueckert[1]

[1] Department of Computing, Imperial College London, U.K,
[2] Guy's Hospital, King's College London, U.K.

Abstract. Radio-frequency (RF) ablation uses electrode-catheters to destroy abnormally conducting myocardial areas that lead to potentially lethal tachyarrhythmias. The procedure is normally guided with x-rays (2D), leading to errors in location and excessive radiation exposure. One of our goals is to provide pre- and intra-operative 3D MR guidance in XMR systems (combined X-ray and MRI room) by locating myocardial regions with abnormal electrical conduction patterns. We address the inverse electro-mechanical relation by using motion in order to infer electrical propagation. For this purpose we define a probabilistic measure of the onset of regional myocardial motion derived from motion fields. The 3D motion fields are obtained using non-rigid registration of tagged MR sequences to track the heart. We also compare regional motion between two different image acquisitions, thus assisting in diagnosing arrhythmia, in follow up of treatment, and particularly in determining whether the electro-physiological intervention succeeded. We validate our methods using an electro-mechanical model of the heart, synthetic data from a cardiac motion simulator for tagged MRI, a cardiac MRI atlas, MRI data from 6 healthy volunteers (one of them subjected to stress), and an MRI study on one patient with tachyarrhythmia, before and after RF ablation. Results seem to corroborate that the ablation had the desired effect of regularising cardiac contraction.

1 Introduction

Advances in non-rigid motion tracking techniques that use tagged MR (SPAMM) now enable us to measure more subtle changes in cardiac motion patterns. One example of disease with associated changes in motion patterns is tachyarrhythmia: a pathological fast heart rhythm originating either in the atria (supraventricular) or ventricles (ventricular), often the result of abnormal paths of conduction. Radio-frequency (RF) ablation is the indicated treatment for patients with life threatening arrhythmia as well as for those on whom drug treatment is ineffective. Applying a RF current via an ablation electrode induces hyperthermia and destruction of the abnormally conducting areas. These procedures are typically carried out under x-ray (2D) guidance, leading to errors in

the location of the abnormal areas as well as to excessive x-ray exposure for the patient.

One of our goals is to provide pre- and intra-operative 3D MR guidance [1] [2] in XMR systems (combined X-ray and MRI room) by detecting the onset of regional motion and relating it to the electrical activation pattern. For this purpose in this work we define a probabilistic measure of regional motion activation derived from a 3D motion field extracted by using non-rigid 3D registration of tagged MR image sequences. Since we address the inverse electro-mechanical problem, trying to infer time of electrical activation by extracting information from the cardiac motion, we use a cardiac atlas and an electro-mechanical model of the heart to validate these results.

The other goal of this work is to detect changes in the regional motion patterns between two different image acquisitions. The purpose of this being the follow up of medical treatment in general, and in particular of patients that have undergone RF ablation. For these patients the method can aid in the identification and localisation of abnormal or changing motion patterns, and also can help determine whether the ablation had the desired effect of regularising cardiac contraction. We use pre- and post-intervention MR images (as well as healthy volunteers and synthetic data) in order to validate this methodology.

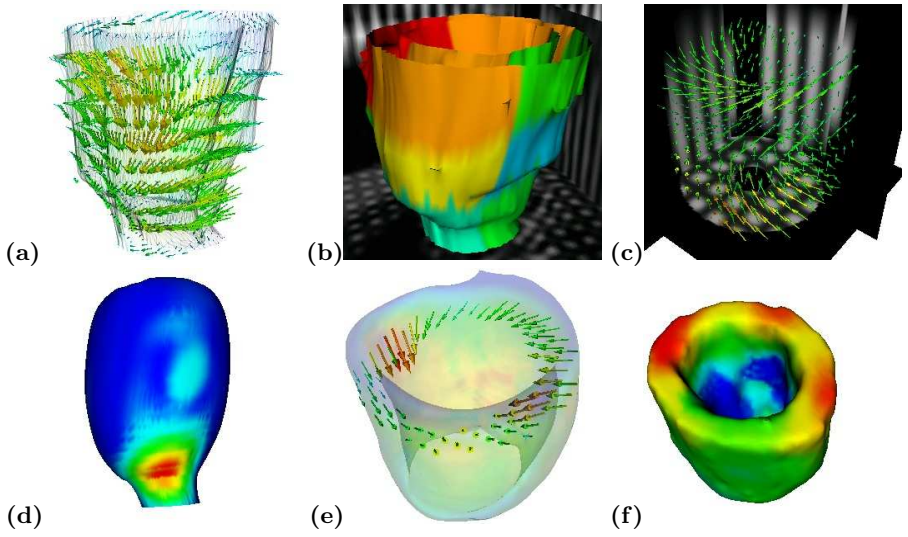

Fig. 1. The reconstructed motion field is shown in **(a)** with displacement vectors and the myocardial surface. The end-diastole myocardial surface ($t = 0$) of a volunteer is shown in **(b)** with the subdivision in 12 segments. In **(c)** the synthetic tagged MR data is displayed with the recovered displacement field while the reconstructed surface in **(d)** is coloured with the magnitude of the difference between the normal and modified parameters. The region where the abnormal motion was produced was accurately identified and can be seen in red and yellow. The smooth cardiac atlas geometry and a slice of its motion field are shown in **(e)**. **(f)** shows the isochrones (time of activation) produced with the electro-mechanical model. All colour scales go from blue to red.

2 Methods

2.1 Registration for motion tracking

We use a non-rigid registration algorithm [3] to track the motion and deformation of the heart in a sequence of 3D short- and long-axis tagged MR images. The goal of the non-rigid registration is to align each time frame of the tagged MR image sequence with the end-systolic (ES) time frame of the image sequence by maximising the normalised mutual information of both time frames. To model cardiac motion we use a free-form deformation based on cubic B-splines. The output of the registration is a continuous time varying 3D motion or vector field (see Figure 1a), $\mathbf{F}(\mathbf{p}, t)$ where $\mathbf{F} : \Re^4 \rightarrow \Re^3$ and $\mathbf{p} \in \Re^3$ is the space coordinate (or voxel (x, y, z) in the discrete implementation).

2.2 Coordinate system and myocardial segmentation

A manual segmentation of the myocardium at end-diastole (ED) (see Figure 1b) is used to determine the region of interest (**myo**) for the registration at time $t = 0$. Using $\mathbf{F}$, the myocardial region can then be automatically propagated over the entire cardiac cycle (as in Figure 1a).

In order to be able to compare different image acquisitions, a common (cylindrical) coordinate system based on the left ventricle is defined for each subject. In this manner we avoid potential misregistration errors due to subject motion between scans. Using cylindrical coordinates based on the LV allows us to express the non-rigid motion measurements derived from $\mathbf{F}$ in terms of radial, circumferential and longitudinal directions.

Using this coordinate system, the myocardium **myo** is then subdivided into small meaningful regions or segments s, and the motion derived measurements for each of these myocardial segment is computed during the cardiac cycle. For the purpose of comparing motion between different scans we use $S = 12$ segments, with 4 sections around the z-axis that roughly correspond to septum, lateral, anterior and posterior walls, and 3 sections along the z-axis, corresponding to base, middle region and apex (see Figure 1b).

2.3 Differential motion descriptors and changes in motion patterns

Some differential features derived from the motion field $\mathbf{F}(\mathbf{p}, t)$ can provide an insight of how a specific region of the myocardium is contracting. We write them as the set of functions

$$F^m = F^m(\mathbf{p}, t) \text{ where } m \in \mu = \{D, R, C, Z, \dot{R}, \dot{C}, \dot{Z}, E, r, c, z, \dot{r}, \dot{c}, \dot{z}\} \quad (1)$$

and $F^m : \Re^4 \rightarrow \Re$ are defined as the total deformation or displacement $F^D = ||\mathbf{F}||$, the radial, circumferential and longitudinal components of the deformation (F^R, F^C and F^Z) with respect to the a cylindrical coordinate system and their corresponding time derivatives or velocities ($F^{\dot{R}}$, $F^{\dot{C}}$ and $F^{\dot{Z}}$), the magnitude of the strain matrix $F^E = ||E_{i,j}||$, the radial, circumferential and longitudinal components of the strain (F^r, F^c and F^z), and their time derivatives ($F^{\dot{r}}$, $F^{\dot{c}}$ and $F^{\dot{z}}$), all with respect to the the same cylindrical coordinate system. Although F^D and F^E are not linearly independent of their components in the cylindrical coordinate system, in this work we explore the efficiency of them all as motion descriptors and those that turn out to be of less importance are minimized by the use of the confidence weights w_m defined in Section 2.4.

We use a Lagrangian framework where the transform $\mathbf{F}(\mathbf{p}, t)$ follows, at time t, the position of the 3D voxels $\mathbf{p} \in \mathbf{myo}$ that correspond to the myocardium at time $t = 0$.

The values of $F^m(\mathbf{p}, t)$ are computed for each voxel and the values averaged for each of the myocardial segments s, for all time frames during the cardiac cycle leading to the function

$$F^m(s,t) = \frac{1}{\int_{\mathbf{p}\in s} d\mathbf{p}} \int_{\mathbf{p}\in s} F^m(\mathbf{p},t) d\mathbf{p} \quad \text{for all regions } s \in \mathbf{myo}. \tag{2}$$

In order to evaluate changes in the motion patterns between two data sets $\mathbf{F}_1$ and $\mathbf{F}_2$, for instance those corresponding to pre- and post-ablation scans, the difference between the two functions F_1^m and F_2^m is computed for each segment, integrated over time and normalised using the maximum value of the function for the specific segment. This normalization of the values compensates for the differences in the dynamic behaviour expected in the various regions of the heart (like apex and base for instance). A statistical measure is derived from the above combined quantities [4] and each segment is assigned a measure of motion change and classified as having either no, small or significant changes.

2.4 Activation detection

The underling assumption is that we can relate the onset of regional motion, derived from the images sequences, to the electrical activation. That is, by using the inverse relation of electro-mechanical coupling. Ideally the onset of regional contraction could be inferred from the motion field with a simple measure such as strain. However, because of the limitations imposed by noise, errors and the relatively low space and time resolution of the image acquisition and the extracted motion field, a more robust measure has to be used. For this purpose we investigate the subset of differential descriptors $\mathbf{F}^m$ where $m \in M = \{R, C, Z, \dot{R}, \dot{C}, \dot{Z}, E, \dot{r}, \dot{c}, \dot{z}\}$.

The first step to characterise the regional motion of the heart during the cardiac cycle is to measuring a regional ($T_{ES}(s)$) and global (T_{ES}) end-systolic times, as well as the critical times for each motion descriptor. We therefore define

$$T^m_{max}(s) = t^* \; such\, that \;\; F^m(s,t^*) \geq F^m(s,t) \quad \forall\, t \in [0, T_{ES}(s)]$$

and

$$T^m_{min}(s) = t^* \; such\, that \;\; F^m(s,t^*) \leq F^m(s,t) \quad \forall\, t \in [T^m_{max}(s), T_{ES}(s)].$$

Notice that for T^m_{min} the search interval begins at T^m_{max}, *i.e.* when the maximum value has been reached (it is the late minimum value of F^m that will help us define the end-systolic time, not those small values at the beginning of the cycle). Because the computation of these values requires a first estimate of the end-systolic time, we use as initialisation the time frame where the heart visually appears to be at end-systole. However, a short iterative process rapidly provides a better estimate for $T_{ES}(s)$.

In the case of displacement and strain, the end-systolic time is linked to their maximum values, while in the case of velocity and rate of change of strain it corresponds to their minimum values (when the heart has paused its contraction).

Therefore,

$$T^m_{ES}(s) = \begin{cases} T^m_{max}(s) & \text{for } m \in \{R, C, Z, E\} \\ \\ T^m_{min}(s) & \text{for } m \in \{\dot{R}, \dot{C}, \dot{Z}, \dot{r}, \dot{c}, \dot{z}\} \end{cases} \tag{3}$$

and combining these times we obtain an estimate that corresponds to the regional time of end-systole:

$$T_{ES}(s) = \sum_{m \in M} w_m T^m_{ES}(s).$$

The weights w_m are normalised (*i.e.* $\sum_{m \in M} w_m = 1$) and reflect the confidence we have on each of the differential motion descriptors m. Although at present we have assigned their values manually, a statistical measure derived from the data is being developed in order to compute them automatically. In order to obtain a global estimate for end-systolic time for each feature we integrate those values over the entire myocardium: $T_{ES} = \int_{s \in \mathbf{myo}} T_{ES}(s) ds$.

Using the above equations we can now define a probabilistic measure of the activation for every voxel in the myocardium, at anytime time during the cardiac cycle:

$$A(s,t) = \sum_{m \in M} w_m \int_0^t \frac{F^m(s,\tau)}{\int_0^{T^m_{max}(s)} F^m(s,\tau')d\tau'} d\tau \tag{4}$$

where we impose $F^m(s,t) = 0$ if $t > T^m_{max}(s)$ in order to keep the values normalised (notice that some motion descriptors like the velocities and the time-derivatives of strain reach their maximum values before end-systole).

The value of $A(s,t)$ monotonically increases from zero to one as we expect every voxel to have been activated by the time the motion descriptors reach the maximum value at time $T^m_{max}(s)$. In order to avoid singularities in the equation we excluded from the computation, and labelled as not active, those voxels that might remain relatively static (*i.e.* those for which $F^m(s, T^m_{max}(s)) \approx 0$).

By integrating over time we obtain an accumulated probability and we can therefore set a (percentage) threshold P, between 0 and 1, to define the time t_a at which the activation of a voxel s takes place. That is, if $A(s,t_a) = P$ then s becomes active for $t = t_a$. An *isochrones* representation is then defined for a given threshold P, as the function $A(s) = t_a$, for all $s \in \mathbf{myo}$.

2.5 Cardiac motion simulator for tagged MRI

For the purpose of validating the proposed methodology with a controlled case we also implemented and modified a cardiac motion simulator for tagged MRI [5]. The motion simulator is based on a 13-parameter model of left-ventricular motion developed by Arts *et al.* [6] and is applied to a volume representing the LV that is modeled as a region between two confocal prolate spheres while the imaging process is simulated by a tagged spin-echo imaging equation [7].

A pair of sequences of synthetic tagged LV images was produced in the following manner: first, a 'post-intervention' (normal) sequence was computed using the standard model parameters, and secondly, a 'pre-intervention' (abnormal) sequence for which the motion parameters were modified in a small region of the myocardium. The modification to the parameters consisted mainly in moving the phase of the contraction forward in time and changing the magnitude of the motion. Two such pairs of image sequences were produced, with different abnormal parameters and in different regions of the myocardium. Examples of these synthetic images can be seen in Figure 1.

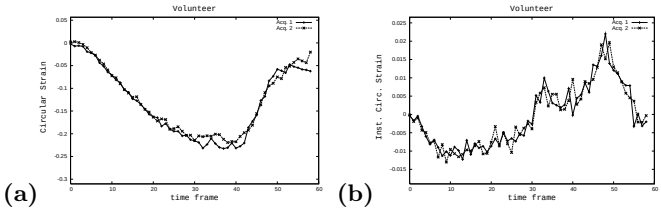

(a) **(b)**

Fig. 2. Reproducibility: Time plots of a typical myocardial segment of a healthy volunteer. The reproducibility of the motion fields is demonstrated with the similar curves obtained for two independent acquisitions of the same subject. The plots show the accumulated **(a)** and instantaneous **(b)** circumferential strain, for each of the two image acquisitions.

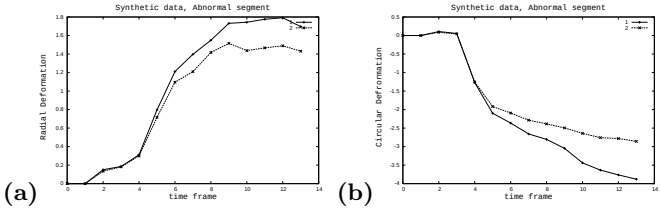

(a) **(b)**

Fig. 3. Synthetic data: Time plots of two segments of the cardiac motion simulator for tagged MRI. Each plot shows results for the normal and modified motion parameters of a segment in the region of abnormal motion, where significant change was correctly detected. The plots show radial **(a)** and circumferential deformation from end-diastole to end-systole.

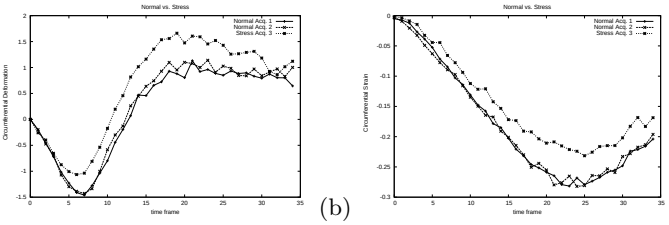

(a) (b)

Fig. 4. Stress study: Time plots of a myocardial segment of a healthy volunteer, with and without stress. There are no significant changes in the motion pattern between the first two image acquisitions. In the third image acquisition, during which stress was induced on the subject, a noticeable alteration was detected. The plots show circumferential deformation **(a)** and strain **(b)** for each of the three image acquisitions.

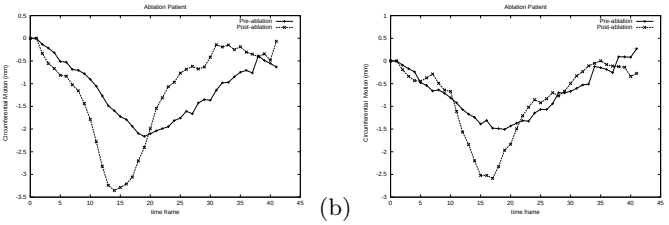

(a) (b)

Fig. 5. RF ablation patient: Time plots of circumferential motion of two myocardial segments of a cardiac patient, before and after RF ablation. A significant change can be seen in the post-intervention sequence, when this region of the myocardium exhibits a faster and more pronounced motion, indicating a regularisation of the contraction.

3 Results and discussion

3.1 Activation detection

Since we are addressing the problem of inverse electro-mechanical coupling, that is, trying to infer the time of electrical activation by extracting information from the cardiac motion images, we have also used a forward 3D **electro-mechanical model** of the heart [8] to validate our results, at this stage in a qualitative manner. The segmentation of the myocardium of a healthy volunteer at end-diastole was used as geometric input for the model. The muscle fiber orientation and the Purkinje network location were fitted to the geometry from a-priori values of the model. Figure 1f shows the isochrones values computed for this subject using the model. Figure 6 compares, in four frames of a sequence, the activation results obtained from Equation 4 and those obtained from the model (in order to simplify visual analysis we display results on the static surface corresponding to end-diastole).

We also used a **cardiac atlas** of geometry and motion generated from 3D MR images sequences of 14 volunteers to test our activation measure in a realistic but smooth and virtually noise-free data set [9] (see Figure 1e). For the purpose of comparing activation detection results to those obtained with the high-resolution electro-mechanical model a larger number of segments was used. Figure 7 compares the isochrones for the atlas computed by both, the electro-mechanical model, and the proposed activation measure derived from the motion field. Promising qualitative agreement can be seen on these preliminary results of activation detection and further validation including direct comparison for stress and ablation data will be ready by the time of the meeting.

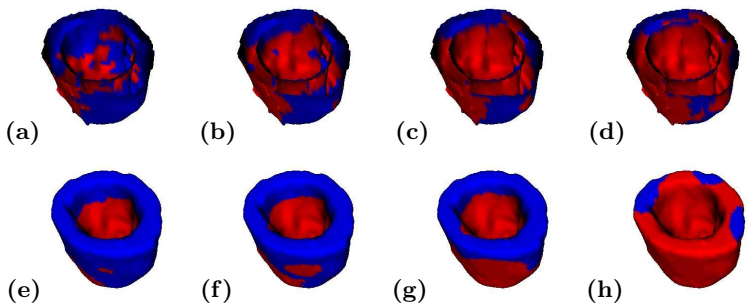

Fig. 6. Activation sequence on the myocardium. Each column correspond to a different time during the cardiac cycle. Blue and red show not active and active voxels, respectively. Images on the top row correspond to results obtained from the motion fields. Those on the bottom row were obtained with the electro-mechanical model. The geometry was interpolated and the top of the myocardial surface was closed to obtain higher resolution for the model.

3.2 Changes in regional motion patterns

The detection of changes in motion patterns was evaluated on synthetic data as well as real MR data from six subjects. In order to test the algorithm when the ground truth is available, results on the 'pre-' and 'post-intervention' sequences of **synthetic** tagged LV images were compared in two cases, with different parameters and regions of abnormal motion (see one case in Figure 1c). In both cases

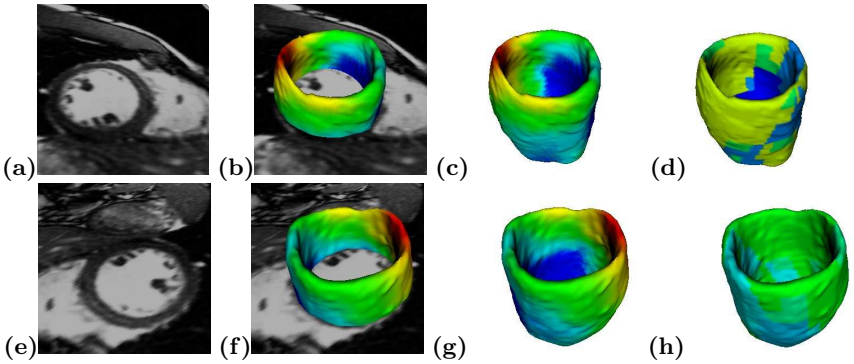

Fig. 7. Isochrones on cardiac atlas. Two views (top and bottom row) of the isochrones were computed for the atlas using both, the electro-mechanical model **(b)**, **(c)**, **(f)** and **(g)**, and the proposed activation measure derived from the motion field **(d)** and **(h)**. The colour scale goes from blue to red, where blue shows the earliest time and red the latest. The orientation of the left and right ventricle can be seen on the MR images of the subject used as a reference for the atlas (**(a)** and **(e)**).

these regions were accurately located. One segment showed significant changes while the rest were correctly classified as having no change (see Figures 1d and 3).

We also acquired data from four volunteers. For each of them two separate sets of image sequences were acquired with only few minutes between the acquisitions. Since no change is expected in these pairs of image acquisitions, this allowed us to verify the **reproducibility** of the motion fields computed by the algorithm and to test the comparison method against false positive detection. The motion patterns encountered were all very similar and no region was classified as having a significant change (see Figure 2).

With another volunteer we acquired three sets of image sequences. The first two as described above, with only few minutes between the acquisitions. The third data set was acquired few minutes after the second, but while subjecting the volunteer to **stress**. The stress was induced by placing one foot of the subject into a bucket of cold water with ice. This experiment allowed us to compare normal motion patterns with those obtained under stress, and again, to validate the method regarding reproducibility and false positives. No segment showed a significant difference between the first two acquisitions, but when comparing normal motion to that under stress we found that three segments showed no change, four presented small but noticeable changes, and the remaining five showed a significant amount of change (see Figure 4).

Finally, MRI data was acquired from an eight year old patient with acute super-ventricular tachyarrhythmia, before and after **RF ablation**. The image acquisition and catheter intervention were carried out with an XMR system [1]. Our results confirmed that the motion pattern changed in most parts of the myocardium (visual inspection of the reconstructed 3D surfaces and displacement vectors also showed pronounced changes in the overall contraction pattern), while the largest changes were found in five segments. Examples of the compared motion also show the corrective effect of the intervention (see Figure 5).

4 Conclusions and future work

In order to account for possible changes in the heart rate between the pre- and post-intervention acquisitions, we intend to re-scale one of the image sequences in the time domain, by using the 4D registration technique described in [9]. Results will be compared to those obtained without rescaling (for instance, in the case of the stress study, where there was a small change in the heart rate).

At present a Markov random field approach is investigated in order to use spatial and time neighbours of every voxel, thus helping decide when does a voxel becomes active, and to make A continuous over space and time.

Despite current limitations such as distingusiging between epi- and endocardial activation patterns, the methodology seems promising for the assessment of intervention results and could also be used for the detection of arrhythmia, ischaemia, regional disfunction and follow up studies in general.

References

[1] K.S. Rhode, D.L.G. Hill, P.J. Edwards, J. Hipwell, D. Rueckert, G.I. Sanchez-Ortiz, S. Hegde, V. Rahunathan, and R. Razavi. Registration and tracking to integrate X-ray and MR images in an XMR facility. *IEEE Transactions on Medical Imaging*, 22(11):1369– 1378, 2003.

[2] G.I. Sanchez-Ortiz, M. Sermesant, R. Chandrashekara, K.S. Rhode, R. Razavi, D.L.G. Hill, and D. Rueckert. Detecting the onset of myocardial contraction for establishing inverse electro-mechanical coupling in XMR guided RF ablation. In *IEEE International Symposium on Biomedical Imaging*, Arlington, USA, 2004.

[3] R. Chandrashekara, R. H. Mohiaddin, and D. Rueckert. Analysis of myocardial motion in tagged MR images using non-rigid image registration. In *Proc. SPIE Medical Imaging 2002: Image Processing*, pages 1168–1179, San Diego, CA, Feb 2002.

[4] G. I. Sanchez-Ortiz, R. Chandrashekara, K.S. Rhode, R. Razavi, D.L.G. Hill, and D. Rueckert. Detecting regional changes in myocardial contraction patterns using MRI. In *SPIE Medical Imaging*, San Diego, USA, Feb 2004.

[5] E. Waks, J. L. Prince, and A. S. Douglas. Cardiac motion simulator for tagged MRI. In *IEEE Workshop on Mathematical Methods in Biomedical Image Analysis*, pages 182–191, San Francisco, CA, 1996.

[6] T. Arts, W. C. Hunter, A. Douglas, A. M. M. Muijtjens, and R. S. Reneman. Description of the deformation of the left ventricle by a kinematic model. *Biomechanics*, 25(10):1119–1127, 1992.

[7] J. L. Prince and E. R. McVeigh. Motion estimation from tagged MR images. *IEEE Transactions on Medical Imaging*, 11(2):238–249, June 1992.

[8] M. Sermesant, K.S. Rhode, S. Hegde, G.I. Sanchez-Ortiz, D. Rueckert, P. Lambiase, C.A. Bucknall, D.L.G. Hill, and R. Razavi. Electromechanical Modelling of the Myocardium using XMR Interventional Imaging. In *Proc. of the Society for Cardiovascular Magnetic Resonance*, Barcelona, Spain, Feb 2004.

[9] D. Perperidis, M. Lorenzo-Valdes, R. Chandrashekara, R. Mohiaddin, G. I. Sanchez-Ortiz, and D. Rueckert. Building a 4D atlas of the cardiac anatomy and motion using MR imaging. In *IEEE International Symposium on Biomedical Imaging*, Arlington, USA, 2004.